Current Science
CS 5 (4), 4209-4218 (2025)
Received 23 May 2025 | **Revised 25 June** 2025 | **Accepted 19 July**. 2025 | **Online Available 30 August** 2025
https://doi.org/ 10.52845/CS/2025-5-4-68

Current Science
Current Science

OPEN ACCESS

ISSN(O) 2795-8639

Original Article

Effect of a MPK Expression Regulation on Biological Behavior and Metabolic Reprogramming in Cervical Cancer Cells

Rouzi Nuermanguli[1], Jiangying Yan[1], Shuhong Zhou[1], Chuan Yang[2*]

[1]Department of Gynecology, Guangyuan Central Hospital,Guangyuan 628000, China

[2]Department of Oncology, Guangyuan Central Hospital,Guangyuan 628000, China

[*]Corresponding Author: Chuan Yang

Abstract:

Background As a key energy metabolism regulator, AMPK is involved in multiple malignancies. This study aimed to explore AMPK's role in cervical cancer metabolic reprogramming.

Methods RNA interference modulated AMPK expression in SiHa cells. Quantitative RT-PCR, CCK-8, wound healing, Transwell, flow cytometry, Western blot, targeted metabolomics, and transmission electron microscopy were used to assess cell behavior, protein expression, metabolism, and ultrastructure.

Results Knockdown of AMPK expression promotes cell proliferation, and with the prolongation of time, its proliferation-promoting effect gradually strengthens. Meanwhile, it enhances cell migration (with a 45.3% increase, $p < 0.001$) and invasion (with a 38.7% increase, $p < 0.001$), and reduces the apoptosis rate (with a 32.6% decrease, $p < 0.01$). AMPK-regulated cells exhibited enhanced proliferative and invasive capacities compared to control cells. Electron microscopic analysis revealed substantial AMPK-mediated alterations in cellular morphology and apoptosis-associated ultrastructures. Metabolomic profiling further corroborated AMPK inhibition-induced metabolic alterations, notably in linoleic acid metabolism (2.3-fold upregulation, $p < 0.001$) and niacin/nicotinamide metabolic pathways (1.8-fold downregulation, $p < 0.01$).

Conclusions This study systematically clarified AMPK's regulatory role in cervical cancer cell metabolic reprogramming, affecting proliferation, migration, invasion, and apoptosis. Findings advance understanding of cervical cancer mechanisms and support AMPK-targeted therapies.

Keywords: Cervical cancer; AMPK; Metabolic reprogramming; Cell proliferation; Invasion; Metabolomics

Introduction

Cervical cancer remains one of the most prevalent malignancies affecting women globally, with increasing incidence and mortality rates observed in certain regions, particularly in underdeveloped areas of China [1-3]. The etiology of cervical cancer is multifaceted, involving the interplay of various factors. Human papillomavirus (HPV) infection is widely acknowledged as the primary etiological factor in cervical carcinogenesis [4-6]. Despite significant advancements in cervical cancer treatment modalities, including surgery, radiotherapy, and chemotherapy, as well as the gradual implementation of novel targeted therapies and immunotherapies in clinical practice, the prognosis for patients with advanced cervical cancer remains poor [7, 8]. Lymph node metastasis control continues to pose a significant clinical challenge and represents a critical factor contributing to disease progression and treatment failure [9].

Metabolic reprogramming in tumor cells is a hallmark feature that sustains their malignant phenotype [10]. This metabolic alteration extends beyond modifications in energy and glucose metabolism, encompassing a systematic remodeling of multiple cellular metabolic

pathways. This reprogramming aims to balance energy supply and biomacromolecule synthesis, thereby providing the essential material foundation for rapid tumor cell proliferation. A comprehensive understanding of this process is crucial for the development of novel therapeutic strategies [11].

Adenosine 5'-Monophosphate Activated Protein Kinase (AMPK) serves as a central regulator of cellular energy metabolism and plays a pivotal role in maintaining cellular energy homeostasis [12]. In recent years, the role of AMPK in tumor biology has garnered significant attention. In cervical cancer, AMPK activation has been reported to inhibit tumor cell proliferation, induce cell cycle arrest, and potentially promote cell apoptosis [13, 14]. Furthermore, AMPK influences tumor cell energy supply by regulating fatty acid metabolism, including the inhibition of fatty acid synthesis and promotion of β-oxidation [15]. AMPK has also been demonstrated to suppress cancer cell migration and invasion, modulate the tumor microenvironment, and affect cell proliferation through signaling pathways such as mTOR [16]. Additionally, AMPK activation can promote autophagy, which may represent a crucial mechanism for maintaining cellular homeostasis [17].

Although existing studies have elucidated the multifaceted role of AMPK in tumor biology, its specific function and molecular mechanisms in the metabolic reprogramming of cervical cancer remain incompletely understood. In light of this, the present study aims to systematically explore the regulatory effects of AMPK on the biological functions of cervical cancer cells, with particular emphasis on its role in the metabolic remodeling process. We hypothesize that AMPK may influence the proliferation, invasion, and metastasis of cervical cancer cells by regulating key metabolic pathways. By gaining a deeper understanding of the role of AMPK-mediated metabolic reprogramming in cervical cancer progression, we aim to provide new insights into the pathogenesis of cervical cancer and establish a theoretical foundation for the development of targeted therapeutic strategies.

2.Materials and Methods

2.1 Cell Culture

The human cervical cancer SiHa cell line (HPV16 positive) was obtained from Wuhan Punosai Biotechnology Co., Ltd. (Wuhan, China). Cells were maintained in MEM complete medium (Gibco, Cat. No. C11095500BT) supplemented with 10% fetal bovine serum (Procell, Cat. No. 164210) and 1% penicillin-streptomycin (Hyclone, Cat. No. SH30010) at 37°C in a humidified atmosphere containing 5% CO2.

2.2 RNA Interference and Quantitative RT-PCR

The sequences of three pooled siRNAs targeting AMPK, designed by Qingke Bio (Bei jing), are presented in Table 1. Transfection was conducted using Lipofectamine 3000 reagent (Invitrogen, Carlsbad, CA, USA) following the manufacturer's protocol. The transfection efficiency was assessed by quantitative RT-PCR, and the siAMPK with the most significant knockdown efficiency was selected for subsequent studies. Total RNA was isolated using TRIzol reagent (Invitrogen, Carlsbad, CA, USA), and qRT-PCR was performed using SYBR Green qPCR SuperMix (Vazyme, Nanjing, China). PCR amplification was carried out using the ABI PRISM 7500 Sequence Detection System (Applied Biosystems, Foster City, CA, USA). The primer sequences are listed in Table 2. The PCR thermal cycling conditions were as follows: initial denaturation at 95°C for 30 seconds, followed by 40 cycles of denaturation at 95°C for 5 seconds and annealing/extension at 60°C for 34 seconds. Each sample was analyzed in triplicate. The relative expression level was calculated using the 2^-ΔΔCt method, with GAPDH serving as the internal reference gene.

Table 1. The RNA interference target sequences

Gene		Sequence(5′-3′)
siAMPK-1	Sense	GAAGAUCGGCCACUACAUU
	Antisense	AAUGUAGUGGCCGAUCUUC
siAMPK-2	Sense	GCUUGAUGCACACAUGAAU
	Antisense	AUUCACUGUGUGCAUCAAGC
siAMPK-	Sense	CCUUUCUGGUGUGGAUUAU

3	Antisense	AUAUCCACACCAGAAAGG
siNC	Sense	UAGCGACUAAACUAUUGU
	Antisense	ACAAUAGUUUAGUCGCUA

TABLE 2. qRT-PCR primer sequences

Gene	Orientation	Sequences(5′-3′)
AMPK	Forward	ACCCATATTATTTGCGTGTA
	Reverse	GTCCCTGATTTGGCTTCT
ACC1	Forward	GCGGAGTGGCTAGAGAAACA
	Reverse	TCCATGGCAACCTCTGGATT
CPT1	Forward	ATGCCATGGATCTGCTGTAT
	Reverse	AGCAGAGTGGAATCGTGGAT
18s	Forward	CCTGGATACCGCAGCTAGGA
	Reverse	GCGGCGCAATACGAATGCCCC

2.3 Cell Proliferation Assay

Cell proliferation was evaluated using the Cell Counting Kit-8 (CCK-8, Bio-Tech, Cat. No. C0037) assay. SiHa cells (4×10^3) were seeded into 96-well plates. At 0, 24, 48, 72, and 96 hours post-seeding, 10 µl of CCK-8 solution was added to each well and incubated at 37°C for 1 hour. The absorbance was measured at a wavelength of 450 nm using a microplate reader. Five replicate wells were used for each time point, and the experiment was performed in triplicate.

2.4 Cell Migration Assay

A uniform horizontal line was inscribed on the reverse side of a 6-well plate, and the surface was coated with 50 µl of fibronectin (10 µg/ml) overnight at 4°C. A cell suspension (1×10^6 cells/ml) was seeded and cultured until a confluent monolayer was formed. Subsequently, cells were treated with mitomycin C (2 µg/ml) for 1 hour to inhibit proliferation. A sterile pipette tip was used to create a scratch wound, and the wells were rinsed with PBS before adding serum-free medium. Images were captured at 0, 6, 24, and 48 hours to document wound healing. The scratch width was measured using Image Pro-Plus software, and the cell migration rate was calculated.

2.5 Transwell Invasion Assay

Matrigel (BD Biosciences) was thawed overnight at 4°C and diluted 1:3 with pre-chilled serum-free medium. 40 µL of the diluted Matrigel was added to pre-chilled Transwell inserts (8 µm pore size, BD Biosciences) and incubated at 37°C for 2 hours to allow gel formation. Cells (1×10^5) suspended in 100 µL serum-free medium were seeded in the upper chamber, while 600 µL of complete medium containing 10% FBS was added to the lower chamber. After 48 hours of incubation, non-invaded cells were removed from the upper surface of the membrane. Invaded cells on the lower surface were fixed and stained with crystal violet. Five random fields per insert were imaged and quantified.

2.6 Cell Apoptosis Assay

Cell apoptosis was analyzed using the Annexin V-FITC Apoptosis Detection Kit (Keygen Biotech, Nanjing, China; Cat. No. KGA106). Harvested cells were resuspended in 1× binding buffer at a concentration of 1×10^6 cells/mL. A 500 µL aliquot of the cell suspension was incubated with 1.25 µL Annexin V-FITC at room temperature in the dark for 15 minutes. Subsequently, 10 µL of propidium iodide was added, and the samples were analyzed within 1 hour using a BD FACSCalibur flow cytometer (BD Biosciences). Data analysis was performed using FlowJo software (Tree Star Inc., Ashland, OR, USA).

2.7 Transmission Electron Microscopy

Cells (1×10^6) were seeded in each well of a 6-well plate. Treated cells were pre-fixed with a mixture of 0.03% glutaraldehyde and 1.5% paraformaldehyde, followed by post-fixation with 1% osmium tetroxide-1.5% potassium ferrocyanide. Samples were then dehydrated, embedded, and sectioned (60-80 nm). Ultrathin sections were double-stained with uranyl acetate and lead citrate. Cell ultrastructure was examined using a JEM-1400 Plus transmission electron microscope (JEOL, Tokyo, Japan).

2.8 Western Blot Analysis

Cells were lysed in RIPA buffer (50 mM Tris-HCl pH 7.4, 150 mM NaCl, 1% NP-40, 0.5% sodium deoxycholate) supplemented with protease inhibitors. Equal amounts of protein (30 μg) were separated by 10% SDS-PAGE and transferred to PVDF membranes (Millipore, Burlington, MA, USA). The membranes were blocked with 5% nonfat milk and incubated with primary antibodies against AMPK, ACC, and CPT1 (1:1000 dilution, Southern Biotech, Birmingham, AL, USA) at 4°C overnight. The membranes were then incubated with HRP-conjugated secondary antibodies (1:5000, Southern Biotech) for 1h at room temperature and developed by ECL chemiluminescence. GAPDH was used as an internal loading control. Band intensities were quantified using ImageJ software (NIH, Bethesda, MD, USA). To ensure the reproducibility and reliability of the results, we performed three independent experimental repeats.

2.9 Non-Targeted Metabolomics Analysis

Cellular metabolite extraction: Cultured cells were washed twice with ice-cold PBS, and 500 μL of a 1:1 (v/v) methanol:acetonitrile mixture was added. The samples underwent three rapid freeze-thaw cycles using liquid nitrogen, followed by sonication for 10 minutes at 4°C. After incubation at -20°C for 1 hour, the samples were centrifuged at 17,000 × g for 15 minutes at 4°C. The supernatant was collected, vacuum-dried using a SpeedVac concentrator, and resuspended in 100 μL of 50% aqueous methanol. LC-MS/MS analysis: LC-MS/MS analysis was performed using a Waters ACQUITY UPLC system (Waters Corporation, Milford, MA, USA) coupled with an AB SCIEX Triple TOF 5600 mass spectrometer (AB SCIEX, Framingham, MA, USA). Chromatographic separation was achieved on an ACQUITY UPLC HSS T3 column (2.1 × 100 mm, 1.8 μm particle size) maintained at 40°C. The injection volume was 5 μL. Mobile phase A consisted of 0.1% formic acid in water (positive ion mode) or 2 mM ammonium acetate in water (negative ion mode), while mobile phase B was acetonitrile. A gradient elution was employed with a flow rate of 0.3 mL/min. Mass spectrometry acquisition parameters were as follows: ion source temperature, 650°C; spray voltage, ±5000 V; ion source gas 1, 60 psi; ion source gas 2, 60 psi; and curtain gas, 35 psi. Data were acquired using the information-dependent acquisition (IDA) mode with a mass range of m/z 50-1200. Data analysis: Raw data were processed using the XCMS Online platform (https://xcmsonline.scripps.edu) for peak extraction, alignment, and matching. Multivariate statistical analyses, including principal component analysis (PCA) and partial least squares discriminant analysis (PLS-DA), were performed using SIMCA-P 14.1 software (Umetrics, Umeå, Sweden). Differential metabolites were identified based on accurate mass measurements, MS/MS fragmentation patterns, and comparisons with the HMDB, METLIN, and KEGG databases. Metabolic pathway enrichment analysis was conducted using MetaboAnalyst 4.0 (https://www.metaboanalyst.ca).

2.10 Statistical Analysis

All data are presented as mean ± standard deviation (SD) from at least three independent experiments. Statistical analyses were performed using GraphPad Prism 8.0 (GraphPad Software, San Diego, CA, USA) and SPSS 25.0 (IBM Corp., Armonk, NY, USA) software. Comparisons between two groups were made using the independent sample t-test, while comparisons among multiple groups were conducted using one-way analysis of variance (ANOVA) followed by Tukey's post hoc test. A p-value < 0.05 was considered statistically significant.

3.Results

3.1 Effect of AMPK on SiHa Cell Proliferation

To assess the impact of AMPK on SiHa cell proliferation, cell viability was measured using the Cell Counting Kit-8 (CCK-8) assay. As illustrated in Figure 1A and 1B, cells in the si-AMPK group exhibited significantly enhanced proliferation compared to the siNC control group at 72 and 96 hours post-transfection ($p < 0.001$). This result suggests that AMPK may play a crucial role in inhibiting the proliferation of cervical cancer cells.

3.2 Effect of AMPK on SiHa Cell Migration and Invasion

The impact of AMPK on SiHa cell migration and invasion was evaluated using scratch wound

healing and Transwell invasion assays, respectively. The scratch wound healing assay revealed a significantly higher wound closure rate in the si-AMPK group compared to the siNC group at both 24 and 48 hours post-wounding (Figure 1C and 1D, $p < 0.05$). Similarly, the Transwell invasion assay demonstrated that AMPK silencing significantly increased the number of cells that traversed the Matrigel matrix (Figure 1E and 1F, $p < 0.01$).

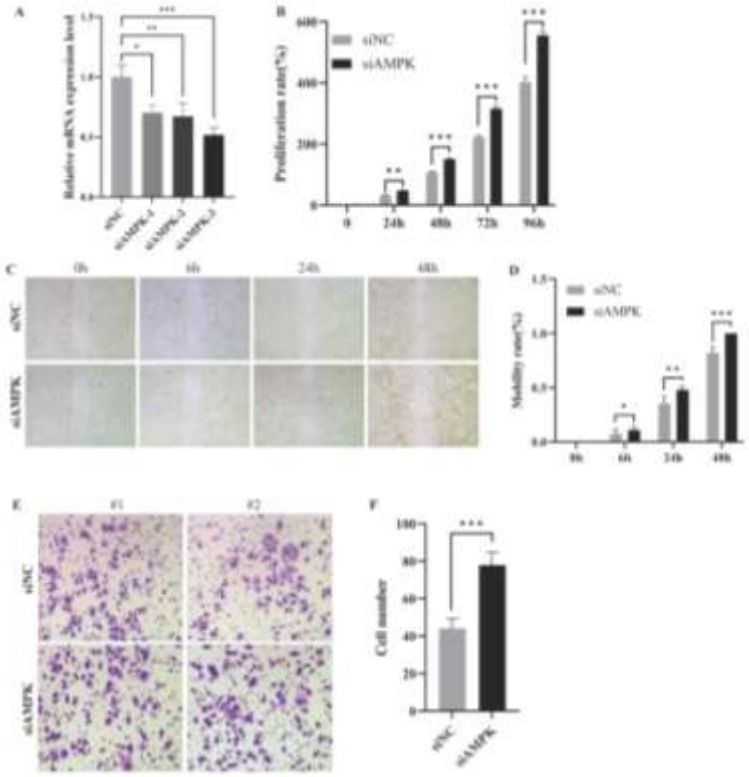

Figure1. Effect of AMPK on SiHa cell proliferation. A, mRNA expression after lentiviral transfection of SiHa cells; B, cck8 assay; C and D, cell scratch assay; E and F, cell transwell assay; (, P < 0.01, ***P < 0.01).**

3.3 Effect of AMPK on SiHa Cell Morphology and Apoptosis

Transmission electron microscopy revealed that SiHa cells in the siNC group exhibited typical apoptotic morphological features, which were less pronounced in the si-AMPK group (Figure 2A). These features included reduced cell volume, cytoplasmic vacuolation, decreased microvilli, aberrant organelle structures, and nuclear chromatin condensation with marginal aggregation. Additionally, late apoptotic cells displayed reduced mitochondrial cristae and enlarged lumina. These observations further support the role of AMPK in promoting SiHa cell apoptosis.

Furthermore, Annexin V-FITC/PI double staining flow cytometry was employed to quantify apoptosis levels. As shown in Figure 2B, the total apoptosis rate (early apoptosis + late apoptosis) in the si-AMPK group was significantly reduced compared to the siNC group (6.16% vs. 15.78%, $p < 0.001$).

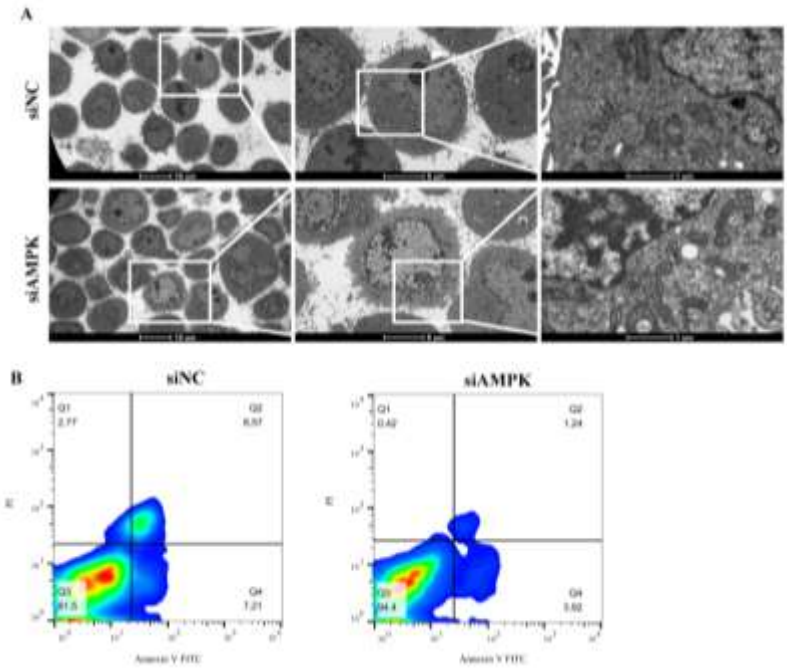

Figure 2. The effect of AMPK on the morphology and apoptosis of SiHa cells. A, Electron microscopy: Each group of images represents different magnifications of the same image, progressing from left to right at 180× (scale bar: 10 μm), 690× (scale bar: 5 μm), and 2900× (scale bar: 1 μm). The magnified regions are marked with white boxes, and the scale bars are shown below each image. B, Flow cytometry: Cell apoptosis.

3.4 Effect of AMPK on the Expression of Genes and Proteins Related to Lipid Metabolism

Western blot analysis revealed that, compared to the siNC group, acetyl-CoA carboxylase 1 (ACC1) protein expression was significantly upregulated in the si-AMPK group, while AMPK and carnitine palmitoyltransferase 1 (CPT1) protein levels were significantly downregulated (Figures 3A and 3B). Quantitative RT-PCR results corroborated this trend, showing significantly decreased AMPK and CPT1 mRNA levels and significantly increased ACC1 mRNA levels in the si-AMPK group (Figure 3C, $p < 0.01$). These findings suggest that AMPK may influence the metabolic state of cervical cancer cells by regulating the expression of key lipid metabolism enzymes.

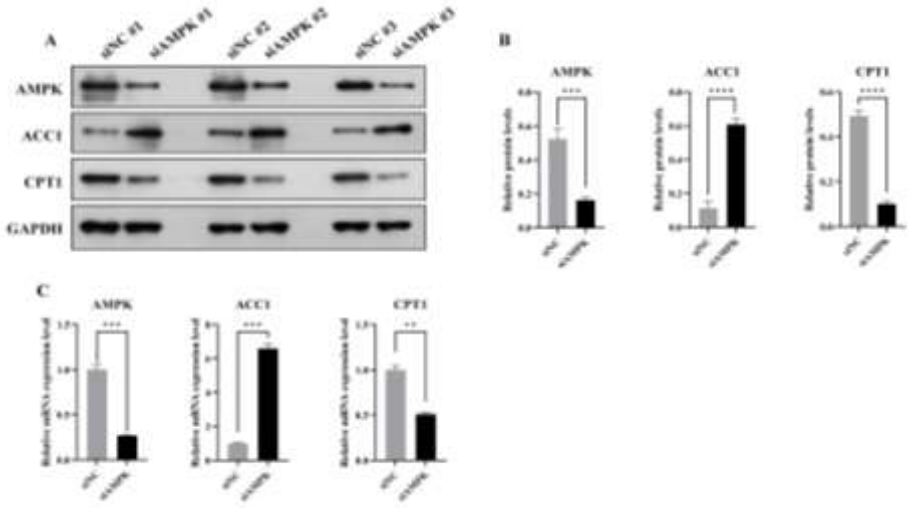

Figure3. Effect of AMPK on the expression of genes and proteins related to lipid metabolism. A and B, relative expression levels of each target protein, the three groups represent three independent experimental repeats; C. mRNA expression; (, P < 0.01, ***P < 0.01, ****, P < 0.0001).**

3.5 AMPK Silencing Leads to Remodeling of the Siha Cell Metabolome

Non-targeted metabolomics analysis revealed significant alterations in the metabolic profile of SiHa cells following AMPK silencing. In the univariate analysis, metabolites with more than 50% missing values were eliminated, and the data were normalized and log-transformed. Volcano plot analysis highlighted significant changes in metabolites between samples. Multivariate analysis using principal component analysis (PCA) demonstrated significant separation between si-NC and si-AMPK group samples (PC1 contribution rate: 77.6%, PC2: 11.7%, Figure 4A). Partial least squares discriminant analysis (PLS-DA) confirmed the significant difference between groups (R2 = 0.588, Q2 = 0.158, Figure 4B). By combining variable importance in projection (VIP) values and t-test results, 71 differential metabolites were identified (Figure 4C-E). KEGG pathway analysis revealed that these metabolites were involved in 8 major metabolic pathways, including linoleic acid metabolism and nicotinate metabolism (Figure 4F). These findings provide new insights and potential therapeutic targets for understanding the role of AMPK in metabolic regulation of cervical cancer.

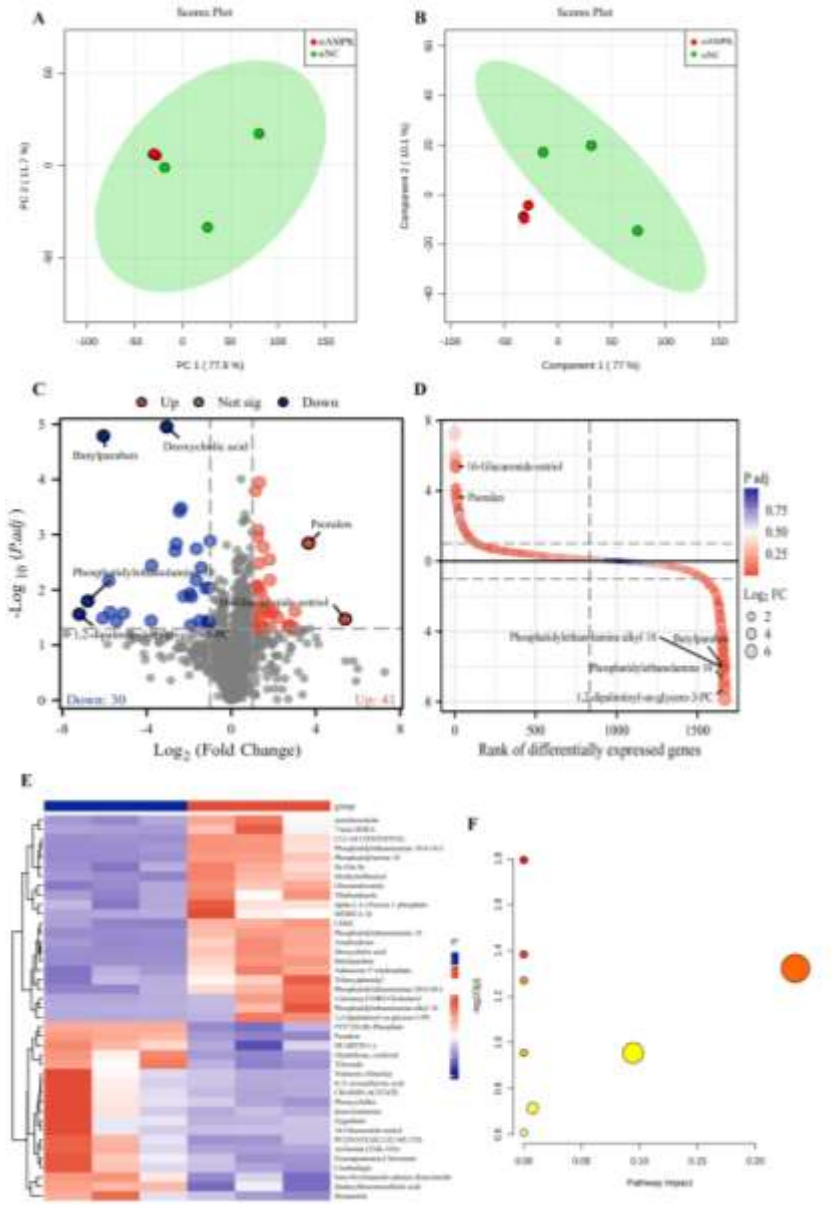

Figure4. AMPK silencing leads to remodeling of the SiHa cell metabolome. A and B, principal component analysis of the two groups of samples; C and D, differential metabolites; E, cluster analysis of differential indicators; F, KEGG metabolic pathway enrichment of differential metabolites; (, P < 0.01, ***P < 0.01, ****, P < 0.0001).**

4 Discussion

Adenosine monophosphate-activated protein kinase (AMPK), a key cellular energy sensor, plays a crucial role in maintaining energy balance and metabolic homeostasis. This study investigated the biological functions and metabolic regulatory mechanisms of AMPK in cervical cancer cells using an siRNA-mediated AMPK knockdown model in SiHa cells, providing valuable insights into AMPK's role in tumor progression.

Our results demonstrated that AMPK downregulation significantly enhanced SiHa cell proliferation, migration, and invasion while suppressing apoptosis. These findings suggest that AMPK may function as a tumor suppressor in cervical cancer, and its loss of function may contribute to enhanced tumor invasiveness and proliferation. AMPK has been shown to regulate cell proliferation and survival through multiple mechanisms, including inhibition of the mTORC1 signaling pathway, regulation of cell cycle progression, and modulation of apoptosis-related protein expression [18, 19]. These mechanisms not only elucidate the multifaceted role of AMPK in tumor suppression but also provide a theoretical foundation for its potential use as a therapeutic target.

Furthermore, our study elucidated the pivotal role of AMPK in regulating lipid metabolism. We observed that AMPK downregulation led to upregulation of ACC1 expression and downregulation of CPT1 expression, consistent with AMPK's established function in lipid metabolism. ACC1, the rate-limiting enzyme for fatty acid synthesis, and CPT1, involved in fatty acid β-oxidation [20, 21], are both regulated by AMPK. AMPK inhibits ACC1 activity through phosphorylation and promotes CPT1 expression, thereby suppressing fatty acid synthesis and promoting fatty acid oxidation [22, 23]. These results suggest that AMPK downregulation may shift tumor cell lipid metabolism towards synthesis, providing essential biomembrane components and energy reserves for rapidly proliferating tumor cells.

Additionally, our metabolomics analysis identified 71 differential metabolites involved in multiple key metabolic pathways, including linoleic acid metabolism and nicotinate metabolism. Notably, the significant alterations in nicotinate and nicotinamide metabolic pathways may reflect adaptive regulation of energy metabolism and redox balance in tumor cells. Nicotinamide, a precursor of NAD+ and NADP+, plays a critical role in cellular energy metabolism, redox homeostasis, and signal transduction [24, 25]. The observed changes in these metabolic pathways offer new perspectives for understanding AMPK's role in tumor metabolic reprogramming.

Despite the significant findings of this study, several limitations should be acknowledged. Firstly, our study primarily relies on in vitro cell models. Future research should include animal experiments and clinical sample analyses to validate AMPK's role in cervical cancer progression. Secondly, AMPK may exhibit diverse functions in different types and stages of cervical cancer, necessitating more comprehensive and in-depth investigations. Lastly, while we observed various metabolic changes induced by AMPK downregulation, the causal relationships between these alterations and tumor cell phenotypes require further elucidation.

5 Conclusion

This study revealed the key role of AMPK in the biological behavior and metabolic regulation of cervical cancer cells, and inhibited tumor cell proliferation, invasion and migration by affecting the levels of a series of small molecule metabolites, providing a basis for the development of new anti-tumor strategies targeting AMPK and its signaling pathway.

Acknowledgements

Not applicable.

Funding

Sichuan Medical Association Project (NO.S2 1057)

Authors' Contributions

Nuermanguli Rouzi and Chuan Yang: overall conception, overall design, review and revision; Nuermanguli Rouzi and Chuan Yang: research conception, experimental implementation, data analysis, paper writing; Shuhong Zhou and Yu Hou: review of some literature, data collection and organization.

Availability of Data and Materials

The data generated in the present study may be requested from the corresponding author. Metabolome sequencing has been uploaded to public databases (URL: www.ebi.ac.uk/metabolights/MTBLS11467).

Ethics approval and consent to participate

Not applicable.

Patient consent for publication

Not applicable.

Competing interest

The authors declare that they have no competing interests.

Reference

1. Han B, Zheng R, Zeng H, Wang S, Sun K, Chen R, et al. Cancer incidence and mortality in China, 2022. Journal of the National Cancer Center. 2024;4(1):47-53. https://doi.org/10.1016/j. jncc.2024.01.006.
2. Li X, Zheng R, Li X, Shan H, Wu Q, Wang Y, et al. Trends of incidence rate and age at diagnosis for cervical cancer in China, from 2000 to 2014. Chinese Journal of Cancer Research. 2017;29(6):477-86. https://doi.org/10.21147/j.issn.1000-9604.2017.06.02.
3. Zhang X, Zeng Q, Cai W, Ruan W. Trends of cervical cancer at global, regional, and national level: data from the Global Burden of Disease study 2019. BMC public health. 2021;21:1-10. https://doi.org/10.1186/s12889-021-10907-5.
4. Molina MA, Steenbergen RDM, Pumpe A, Kenyon AN, Melchers WJG. HPV integration and cervical cancer: a failed evolutionary viral trait. Trends in molecular medicine. 2024;30(9):890-902. https://doi.org/10.1016/j.molmed.2024.05.009.
5. Ong SK, Abe SK, Thilagaratnam S, Haruyama R, Pathak R, Jayasekara H, et al. Towards elimination of cervical cancer - human papillomavirus (HPV) vaccination and cervical cancer screening in Asian National Cancer Centers Alliance (ANCCA) member countries. The Lancet regional health Western Pacific. 2023;39(null):100860. https://doi.org/10. 1016/j.lanwpc.2023.100860.
6. Lei J, Arroyo-Mühr LS, Lagheden C, Eklund C, Nordqvist Kleppe S, Elfstr?m M, et al. Human Papillomavirus Infection Determines Prognosis in Cervical Cancer. Journal of clinical oncology. 2022;40(14):1522-8. https://doi.org/10.1200/JCO.21.01930.
7. Simms KT, Yuill S, Killen J, Smith MA, Kulasingam S, de Kok I, et al. Historical and projected hysterectomy rates in the USA: Implications for future observed cervical cancer rates and evaluating prevention interventions. Gynecologic oncology. 2020;158(3):710-8. https://doi.org/10.1016/j.ygyno.2020.05.030.
8. Monk BJ, Enomoto T, Kast WM, McCormack M, Tan DS, Wu X, et al. Integration of immunotherapy into treatment of cervical cancer: Recent data and ongoing trials. Cancer treatment reviews. 2022;106:102385. https://doi.org/10.1016/j.ctrv.2022.102385.
9. Bogani G, Maggiore ULR, Rossetti D, Ditto A, Martinelli F, Chiappa V, et al. Advances in laparoscopic surgery for cervical cancer. Critical Reviews in Oncology/Hematology. 2019;143:76-80. https://doi.org/10.1016/j.critrevonc.2019.07.021.
10. Hanahan D, Weinberg RA. Hallmarks of cancer: the next generation. cell. 2011;144 (5): 646-74. https://doi.org/10.1016/j.cell.2011.02.013.
11. Faubert B, Solmonson A, DeBerardinis RJ. Metabolic reprogramming and cancer progression. Science. 2020;368(6487): eaaw 5473. https://doi.org/10.1126/science.aaw5473.
12. Herzig S, Shaw RJ. AMPK: guardian of metabolism and mitochondrial homeostasis. Nature reviews Molecular cell biology. 2018;19(2):121-35. https://doi.org/10.1038/nrm.2017.95.
13. Konieczny P, Adamus T, Sulkowski M, Skrzypek K, Majka M. Impact of AMPK on cervical carcinoma progression and metastasis. Cell Death & Disease. 2023;14(1):43. https://doi.org/10.1038/s41419-023-05583-9.
14. Yung MMH, Chan DW, Liu VWS, Yao K-M, Ngan HY-S. Activation of AMPK inhibits cervical cancer cell growth through AKT/FOXO3a/FOXM1 signaling cascade. BMC cancer. 2013;13:1-8. https://doi.org/10.1186/1471-2407-13-327.
15. O'Neill HM, Holloway GP, Steinberg GR. AMPK regulation of fatty acid metabolism and mitochondrial biogenesis: implications for obesity. Molecular and cellular endocrinology.

2013;366(2):135-51. https://doi.org/10.1016/j.mce.2012.06.019.
16. Zhang L, Liu W, Liu F, Wang Q, Song M, Yu Q, et al. IMCA induces ferroptosis mediated by SLC7A11 through the AMPK/mTOR pathway in colorectal cancer. Oxidative medicine and cellular longevity. 2020;2020 (1):1675613. https://doi.org/10.1155/2020/1675613.
17. Sun D, Tao W, Zhang F, Shen W, Tan J, Li L, et al. Trifolirhizin induces autophagy-dependent apoptosis in colon cancer via AMPK/mTOR signaling. Signal transduction and targeted therapy. 2020;5(1):174. https://doi.org/10.1038/s41392-020-00281-w.
18. Ling NX, Kaczmarek A, Hoque A, Davie E, Ngoei KR, Morrison KR, et al. mTORC1 directly inhibits AMPK to promote cell proliferation under nutrient stress. Nature metabolism. 2020;2(1):41-9. https://doi.org/10.1038/s42255-019-0157-1.
19. Xie G, Sun L, Li Y, Chen B, Wang C. Periplocin inhibits the growth of pancreatic cancer by inducing apoptosis via AMPK-mTOR signaling. Cancer Medicine. 2021;10 (1):325-36. https://doi.org/10.1002/cam4.3611
20. Ito H, Nakamae I, Kato J-y, Yoneda-Kato N. Stabilization of fatty acid synthesis enzyme acetyl-CoA carboxylase 1 suppresses acute myeloid leukemia development. The Journal of clinical investigation. 2021;131(12). https://doi.org/10.1172/JCI141529.
21. Schlaepfer IR, Joshi M. CPT1A-mediated fat oxidation, mechanisms, and therapeutic potential. Endocrinology. 2020;161(2):bqz 046. https://doi.org/10.1210/endocr/bqz046.
22. Pang Y, Xu X, Xiang X, Li Y, Zhao Z, Li J, et al. High fat activates O-GlcNAcylation and affects AMPK/ACC pathway to regulate lipid metabolism. Nutrients. 2021;13(6):1740. https://doi.org/10.3390/nu13061740.
23. Fang C, Pan J, Qu N, Lei Y, Han J, Zhang J, et al. The AMPK pathway in fatty liver disease. Frontiers in Physiology. 2022;13:970292. https://doi.org/10.3389/fphys.2022.970292.
24. Maiese K. New Insights for nicotinamide: Metabolic disease, autophagy, and mTOR. Frontiers in bioscience (Landmark edition). 2020;25:1925. https://doi.org/10.2741/4886.
25. Navas LE, Carnero A. Nicotinamide adenine dinucleotide (NAD) metabolism as a relevant target in cancer. Cells. 2022;11(17): 2627. https://doi.org/10.3390/cells11172627.